

**SYNTHESIS, CHARACTERIZATION AND MODIFICATION OF SAPO-34  
ZEOLITE MEMBRANE FOR SEPARATION OF CO<sub>2</sub> FROM BINARY GAS  
MIXTURES**

**by**

**CHEW THIAM LENG**

**Thesis submitted in fulfilment of the  
requirements for the degree of  
Doctor of Philosophy**

**May 2012**

## ACKNOWLEDGEMENTS

First of all, I would like to dedicate my deep gratitude to my supervisor, Professor Subhash Bhatia for his guidance and advice in supervising me throughout the whole Ph.D. degree. He is always supportive in assisting me to solve any problems faced in my research work. I would like to highly appreciate his effort and patience in reading my thesis. I would like to express my sincere thanks to my co-supervisor, Professor Abdul Latif Ahmad for his advice and review during the preparation of my thesis. My dissertation could not be completed without the help from Professor Subhash Bhatia and Professor Abdul Latif Ahmad.

Thanks to all the administrative staffs and laboratory technicians of School of Chemical Engineering, USM, for their friendly help and support without any reluctance. In addition, thanks also to Mr. Karuna and Mr. Hazhar from School of Physics (USM), Mr. Ong Chin Hin, Jamal and Ramlee from School of Chemical Sciences (USM), Mr. Masrul Mansor from School of Biological Sciences (USM), Mr. Rashid and Mr. Hasnor from School of Materials & Mineral Resources Engineering, Dr. Husin from AMREC (Kulim), for their professional helps in analyzing the samples for my research work.

Special thanks to my family for their spiritual support, concern and encouragement. Apart from that, I would like to show my token of appreciation to my friends in USM, especially Dr. Yeong Yin Fong, Dr. Lee Keat Teong, Dr. Low Siew Chun, Dr. Chan Choi Yee, Dr. Oh Pei Ching, Dr. Ooi Boon Seng, Dr. Derek, Dr. Lim Jit Kang, Dr. Leo Choe Peng, Dr. Sim Jia Huey, Dr. Sumathi, Ms. Low Ee Mee, Ms. Wee Shin Ling, Ms. Ang Gaik Tin, Mr. Ong Yit Thai, Mr. Fan Mun Sing,

Mr. Henry Foo, Mr. Tan Kok Tat and Mr. Tan Sek Cheong, for their companionship and helpful advice.

I wish to express my acknowledgement to USM fellowship scheme for the financial support throughout the time of my research work. The fundings provided by USM under FRGS (Account No: 6070021 and 6071214) and RU (Account No: 811043) for conducting the research work are gratefully acknowledged.

Chew Thiam Leng

April 2012

## TABLE OF CONTENT

	Page
<b>ACKNOWLEDGEMENTS</b>	ii
<b>TABLE OF CONTENTS</b>	iv
<b>LIST OF TABLES</b>	xi
<b>LIST OF FIGURES</b>	xiv
<b>LIST OF PLATES</b>	xxi
<b>LIST OF ABBREVIATION</b>	xxii
<b>LIST OF SYMBOLS</b>	xxv
<b>ABSTRAK</b>	xxviii
<b>ABSTRACT</b>	xxix
<b>CHAPTER 1 - INTRODUCTION</b>	1
1.1 Zeolite	1
1.2 Zeolite Membrane	3
1.3 Gas separation	4
1.3.1 Issue of CO <sub>2</sub> Gas Separation	4
1.3.2 Conventional Method for CO <sub>2</sub> Gas Separation	5
1.3.3 Membrane-based CO <sub>2</sub> Gas Separation Technology	6
1.3.4 Zeolite Membrane for CO <sub>2</sub> Gas Separation	9
1.4 Problem Statement	10
1.5 Objectives	15
1.6 Scope of the Study	16
1.6.1 Synthesis of SAPO-34 Zeolite Membranes	16
1.6.2 Modification of SAPO-34 Zeolite Membranes	16
1.6.3 Characterization of Unmodified and Modified SAPO-34 Zeolite Membranes	16
1.6.4 Single Gas Permeation, Binary Gas Mixtures Permeation and Separation using SAPO-34 Zeolite Membranes	17

1.6.5	Optimization for Binary Gas Mixtures Permeation and Separation of Modified SAPO-34 Zeolite Membrane using DOE	18
1.6.6	Modeling for Single Gas Permeation, Binary Gas Mixture Permeation and Separation of Modified SAPO-34 Zeolite Membrane	18
1.8	Organization of Thesis	19
<b>CHAPTER 2 - LITERATURE REVIEW</b>		21
2.1	Synthesis of Zeolite Membrane	21
2.1.1	Methods of Zeolite Membrane Synthesis	22
2.1.1 (a)	Direct in-situ crystallization	30
2.1.1 (b)	Secondary Growth Method	31
2.1.1 (c)	Semi-continuous or Continuous Flow Systems	32
2.1.1 (d)	MW Heating	34
2.1.1 (e)	Dry or Wet Gel Conversion Method	37
2.1.2	Support for Zeolite Membrane	39
2.1.3	Template/SDA Removal by Thermal Treatment	40
2.2	Characterization of Zeolite Membrane	42
2.3	Gas Permeation and Separation	43
2.3.1	Principle for Gas Permeation and Separation	43
2.4	Gas Permeation and Separation using Zeolite Membranes	45
2.4.1	Modes of Gas Permeation and Separation using Zeolite Membranes	45
2.4.2	Single Gas Permeation through Zeolite Membranes	47
2.4.3	Binary Gas Permeation and Separation for Zeolite Membranes	50
2.4.3 (a)	CO <sub>2</sub> /N <sub>2</sub> System	51
2.4.3 (b)	CO <sub>2</sub> /CH <sub>4</sub> System	53
2.4.3 (c)	CO <sub>2</sub> /H <sub>2</sub> System	55
2.5	Modification of Zeolite Membrane	57
2.5.1	Silylation	58
2.5.2	Ion-exchange	58
2.6	Modeling	60
2.7	Closing Remarks	65

<b>CHAPTER 3 - MATERIALS AND METHODS</b>	<b>66</b>
3.1 Materials and Chemicals	66
3.2 Preparation of Membranes	68
3.2.1 Preparation of Membrane Supports	69
3.2.2 Hydrothermal Synthesis of SAPO-34 Membranes	70
3.2.3 Modification of SAPO-34 Membranes	76
3.3 Characterization Studies	79
3.3.1 SEM	79
3.3.2 XRD	79
3.3.3 TEM and SAED	80
3.3.4 TGA	80
3.3.5 FTIR	80
3.3.6 Nitrogen Adsorption-Desorption Measurement	81
3.3.7 Elemental Composition	81
3.3.8 Nitrogen Permeation Test	81
3.4 Gas Permeation and Separation Studies	82
3.4.1 DOE	83
3.4.2 Gas Permeation and Separation Test Rig Setup	85
3.4.3 Gas Permeation Cell	89
3.4.4 Operation of Gas Permeation and Separation Test Rig	91
3.1.1 (a) Check for Test Rig Leakage	91
3.1.1 (b) System Vacuum	92
3.1.1 (c) Single Gas Permeation Studies	93
3.1.1 (d) Binary Gas Permeation and Separation Studies	94
3.4.5 Gas Samples Analysis	96
3.4.6 Gas Permeation and Separation Performance Studies	96
3.5 Modeling Studies	98
3.5.1 Modeling of Single Gas Permeation	99
3.5.2 Modeling of Binary Gas Permeation and Separation	102
3.5.3 Closing Remarks	105

<b>CHAPTER 4 - RESULTS AND DISCUSSION</b>	106
4.1 Characterization of SAPO-34 Zeolite Membrane	107
4.1.1 SAPO-34 Zeolite Membrane	107
4.1.1 (a) SEM	107
4.1.1 (b) Weight Gain of Membranes	116
4.1.1 (c) XRD	118
4.1.1 (d) TEM and SAED	120
4.1.1 (e) TGA	122
4.1.1 (f) FTIR	125
4.1.1 (g) Nitrogen Adsorption-Desorption Measurement	127
4.1.2 Modified SAPO-34 Zeolite Membrane	129
4.1.2 (a) Elemental Composition	129
4.1.2 (b) Nitrogen Adsorption-Desorption Measurement	130
4.2 Preliminary Gas Permeation and Separation Test	131
4.2.1 SAPO-34 Zeolite Membranes	131
4.2.1 (a) Comparison of Preliminary Gas Permeation and Separation Performance of Different Types of Membranes	131
4.2.2 Modified SAPO-34 Zeolite Membranes	135
4.2.2 (a) Comparison of Preliminary Gas Permeation and Separation Performance of Different Types of Membranes	135
4.2.3 Reproducibility Studies of Preparation of MW-2 and Ba-MW-2 Membranes for Gas Permeation and Separation	139
4.2.4 Summary of Preliminary Gas Permeation and Separation Test	142

4.3	Gas Permeation and Separation Studies of Ba-SAPO-34 Membrane	143
4.3.1	Single Gas Permeation Studies of CO <sub>2</sub> , CH <sub>4</sub> , N <sub>2</sub> and H <sub>2</sub>	143
4.3.2	Binary Gas Permeation and Separation Studies of CO <sub>2</sub> /CH <sub>4</sub> Gas Mixture	153
	4.3.2 (a) Effect of Pressure Difference	153
	4.3.2 (b) Effect of Temperature	156
	4.3.2 (c) Effect of Feed Composition (CO <sub>2</sub> Concentration in the Feed)	159
4.3.3	Binary Gas Permeation and Separation Studies of CO <sub>2</sub> /N <sub>2</sub> Gas Mixture	162
	4.3.3 (a) Effect of Pressure Difference	162
	4.3.3 (b) Effect of Temperature	164
	4.3.3 (c) Effect of Feed Composition (CO <sub>2</sub> Concentration in the Feed)	167
4.3.4	Binary Gas Permeation and Separation Studies of CO <sub>2</sub> /H <sub>2</sub> Gas Mixture	169
	4.3.4 (a) Effect of Pressure Difference	169
	4.3.4 (b) Effect of Temperature	172
	4.3.4 (c) Effect of Feed Composition (CO <sub>2</sub> Concentration in the Feed)	175
4.3.5	Gas Permeation and Separation Durability Test of Ba-MW-2 Membrane	177
4.3.6	Comparison of Gas Permeation and Separation Performance of Ba-MW-2 Membrane with Other Zeolite Membranes Reported in the Literature	179
	4.3.6 (a) CO <sub>2</sub> /CH <sub>4</sub> Gas Permeation and Separation	179
	4.3.6 (b) CO <sub>2</sub> /N <sub>2</sub> Gas Permeation and Separation	183
	4.3.6 (c) CO <sub>2</sub> /H <sub>2</sub> Gas Permeation and Separation	185

4.4	DOE	189
4.4.1	Gas Permeation and Separation of CO <sub>2</sub> /CH <sub>4</sub> Gas Mixture	189
4.4.1 (a)	Full Factorial Design	189
4.4.1 (b)	Response of CO <sub>2</sub> Permeance	190
4.4.1 (c)	Response of Separation Selectivity	193
4.4.1 (d)	Optimization using RSM	196
4.4.2	Gas Permeation and Separation of CO <sub>2</sub> /N <sub>2</sub> Gas Mixture	199
4.4.2 (a)	Full Factorial Design	199
4.4.2 (b)	Response of CO <sub>2</sub> Permeance	200
4.4.2 (c)	Response of Separation Selectivity	203
4.4.2 (d)	Optimization using RSM	206
4.4.3	Gas Permeation and Separation of CO <sub>2</sub> /H <sub>2</sub> Gas Mixture	209
4.4.3 (a)	Full Factorial Design	209
4.4.3 (b)	Response of CO <sub>2</sub> Permeance	210
4.4.3 (c)	Response of Separation Selectivity	213
4.4.3 (d)	Optimization using RSM	216
4.5	Modeling Studies for Gas Permeation and Separation through Ba-MW-2 Zeolite Membrane	219
4.5.1	Determination of Adsorption Parameters and Gas Diffusivities	219
4.5.2	Simulated Single Gas Permeation	224
4.5.3	Simulated Binary Gas Mixture Permeation and Separation	231
4.6	Validation of Models for Gas Permeation and Separation through Ba-MW-2 Zeolite Membrane	237
4.7	Closing Remarks	244
<b>CHAPTER 5 -CONCLUSIONS AND RECOMMENDATIONS</b>		246
5.1	Conclusions	246
5.2	Recommendations	248
<b>BIBLIOGRAPHY</b>		249

<b>APPENDICES</b>	
Appendix A.1 Formation of SAPO-34 using direct in-situ crystallization and MW heating	269
Appendix B.1 Data Analysis for the Single Gas Permeation of CO <sub>2</sub> , CH <sub>4</sub> , N <sub>2</sub> and H <sub>2</sub> through Ba-SAPO-34 Zeolite Membrane	271
Appendix B.2 Data Analysis for the Binary Gas Permeation and Separation of CO <sub>2</sub> /CH <sub>4</sub> Gas Mixture through Ba-SAPO-34 Zeolite Membrane	273
Appendix C.1 Solution for Modeling of Single Gas Permeation, Binary Gas Permeation and Separation	279
Appendix D.1 MATLAB Command for Modeling of Single Gas Permeation	286
Appendix D.2 MATLAB Command for Modeling of Binary Gas Permeation and Separation	288
<b>LIST OF PUBLICATIONS</b>	291

## LIST OF TABLES

	Page
1.1 Different zeolite framework structures reported in the literature (Bowen <i>et al.</i> , 2004; Julbe, 2007; Payra and Dutta, 2003)	2
1.2 Characterization techniques of SAPO-34 zeolite membrane	17
2.1 Different types of liquid phase synthesis methods used for the formation of zeolite membranes	26
2.2 The chemicals used in preparation of precursor solution for SAPO-354 materials	29
2.3 Single gas permeances through zeolite membranes	48
2.4 CO <sub>2</sub> /N <sub>2</sub> permeation and separation using zeolite membranes reported in the literature	52
2.5 CO <sub>2</sub> /CH <sub>4</sub> permeation and separation using zeolite membranes reported in the literature	54
2.6 CO <sub>2</sub> /H <sub>2</sub> permeation and separation using zeolite membranes reported in the literature	56
3.1 List of chemicals and reagents used	67
3.2 List of equipment used	68
3.3 Membranes synthesized using direct in-situ crystallization and MW heating in present study	75
3.4 Membranes prepared by ion-exchanging MW-2 membranes with different cations	76
3.5 Process variables ranges studied in the gas permeation and separation studies through the zeolite membrane	83
3.6 List of main components for the gas permeation and separation test rig	87
4.1 Code of the membranes synthesized in present study	106
4.2 Weight gain of different membrane	116
4.3 Reproducibility test for weight gain of membranes	117
4.4 Powder sample weight loss obtained from TGA analysis	124
4.5 IR bands in FTIR spectrum obtained for the HS-24 powder sample	126

4.6	Texture properties of the HS-24 and MW-2 powder sample	128
4.7	Elemental compositions of unmodified and modified membranes	129
4.8	Texture properties of the unmodified and modified powder samples	130
4.9	Preliminary equimolar gas permeation and separation studies at 100 kPa pressure difference and 30 °C for different membranes	132
4.10	Increase in separation selectivities in preliminary equimolar gas permeation and separation studies at 100 kPa pressure difference and 30 °C after modification of MW-2 with different cations	138
4.11	Reproducibility studies of MW-2 membrane preparation for gas permeation and separation	140
4.12	Reproducibility studies of Ba-MW-2 membrane preparation for gas permeation and separation	141
4.13	Physical properties of different gas molecules (Shekhawat <i>et al.</i> , 2003)	143
4.14	Comparison of CO <sub>2</sub> /CH <sub>4</sub> gas permeation and separation performance of Ba-MW-2 membrane and the other reported zeolite membranes	180
4.15	Comparison of CO <sub>2</sub> /N <sub>2</sub> gas permeation and separation performance of Ba-MW-2 membrane and the other reported zeolite membranes	184
4.16	Comparison of CO <sub>2</sub> /H <sub>2</sub> gas permeation and separation performance of Ba-MW-2 membrane and the other reported zeolite membranes	186
4.17	Experiment design matrix and responses for the gas permeation and separation studies of CO <sub>2</sub> /CH <sub>4</sub>	189
4.18	Goals for optimization of CO <sub>2</sub> /CH <sub>4</sub> permeation and separation studies	197
4.19	Optimum condition for the 1/(CO <sub>2</sub> permeance) and 1/(CO <sub>2</sub> /CH <sub>4</sub> separation selectivity)	197
4.20	Verification experiments at optimum operating conditions generated by DOE for the CO <sub>2</sub> /CH <sub>4</sub> permeation and separation studies	199
4.21	Experiment design matrix and responses for the permeation and separation studies of CO <sub>2</sub> /N <sub>2</sub>	200
4.22	Goals for optimization of CO <sub>2</sub> /N <sub>2</sub> permeation and separation studies	207

4.23	Optimum condition for the $1/(\text{CO}_2 \text{ permeance})$ and $1/(\text{CO}_2/\text{N}_2 \text{ separation selectivity})$	207
4.24	Verification experiments at optimum operating conditions generated by DOE for the $\text{CO}_2/\text{N}_2$ permeation and separation studies	208
4.25	Experiment design matrix and responses for the permeation and separation studies of $\text{CO}_2/\text{H}_2$	209
4.26	Goals for optimization of $\text{CO}_2/\text{H}_2$ permeation and separation studies	217
4.27	Optimum condition for the $1/(\text{CO}_2 \text{ permeance})$ and $1/(\text{CO}_2/\text{H}_2 \text{ separation selectivity})$	217
4.28	Verification experiments at optimum operating conditions generated by DOE for the $\text{CO}_2/\text{H}_2$ permeation and separation studies	218
4.29	Adsorption equilibrium constants of different gas molecules on Ba-MW-2 membrane	220
4.30	Heat of adsorption and entropy of adsorption of gas molecules on Ba-MW-2 membrane	222
4.31	M-S diffusivities obtained from single gas fluxes through Ba-MW-2 membrane	223
4.32	Activation energies and infinite M-S diffusivities for diffusion of gas molecules through Ba-MW-2 membrane	224
B.1.1	Measurement of permeate stream flow using bubble flowmeter	271
B.1.2	Calculated single gas fluxes and permeances	272
B.2.1	Flow and composition of different streams in the $\text{CO}_2/\text{CH}_4$ binary gas mixture system	275

## LIST OF FIGURES

	Page
1.1 Schematic of a supported zeolite membrane	4
1.2 Common technologies for CO <sub>2</sub> separation (Li <i>et al.</i> , 2011; Olajire, 2010)	5
1.3 Framework structure of CHA (Li <i>et al.</i> , 2004; IZA-SC, 2008)	10
2.1 Phenomenon occurrence for transformation of nutrients into zeolite crystals (Coronas, 2010)	22
2.2 General methods for synthesis of zeolite membranes (Caro <i>et al.</i> , 2000)	23
2.3 Steps in the preparation of zeolite membranes on double side of disc-shaped support for different methods: (a) direct in-situ crystallization hydrothermal synthesis, (b) secondary growth (seeded) hydrothermal synthesis and (c) vapor phase synthesis	24
2.4 Schematic of continuous system for membrane synthesis (Çulfaz <i>et al.</i> , 2006)	33
2.5 Various membrane permeation and separation mechanism on gaseous mixtures: (a) viscous flow, (b) Knudsen diffusion, (c) molecular sieving, (d) solution diffusion and (e) adsorption / surface diffusion (Lu <i>et al.</i> , 2007)	43
2.6 Effect of temperature of typical permeation through zeolite membrane (Algieri <i>et al.</i> , 2003)	46
2.7 Kinetic diameter of various gas molecules	46
3.1 Heating and cooling profiles for sintering of $\alpha$ -alumina support	69
3.2 Procedures in preparation of the SAPO-34 zeolite membranes and powder samples using direct in-situ crystallization and MW heating	70
3.3 Schematic diagram of gas permeation and separation test rig with GC	85
3.4 Gas permeation cell	91
3.5 Schematic description of gas permeation through the zeolite membrane	99
4.1 XRD patterns of (a) $\alpha$ -alumina disc and (b) HS-24 membrane	118
4.2 XRD patterns of (a) MW-0.5, (b) MW-1, (c) MW-2 and (d) MW-3 membranes	119

4.3	TGA curves of (a) HS-24 and (b) MW-2 zeolite powder samples	123
4.4	FTIR spectrum of (a) MW-0.5, (b) MW-1, (c) MW-2, (d) MW-3 and (e) HS-24 powder samples	125
4.5	Nitrogen adsorption-desorption isotherms of (a) HS-24 and (b) MW-2 zeolite powder samples	127
4.6	Preliminary equimolar CO <sub>2</sub> /CH <sub>4</sub> permeation and separation study at 100 kPa pressure difference and 30 °C for different membranes	133
4.7	Preliminary equimolar CO <sub>2</sub> /N <sub>2</sub> permeation and separation study at 100 kPa pressure difference and 30 °C for different membranes	134
4.8	Preliminary equimolar CO <sub>2</sub> /H <sub>2</sub> permeation and separation study at 100 kPa pressure difference and 30 °C for different membranes	134
4.9	Preliminary equimolar CO <sub>2</sub> /CH <sub>4</sub> permeation and separation study at 100 kPa pressure difference and 30 °C for different membranes	136
4.10	Preliminary equimolar CO <sub>2</sub> /N <sub>2</sub> permeation and separation study at 100 kPa pressure difference and 30 °C for different membranes	136
4.11	Preliminary equimolar CO <sub>2</sub> /H <sub>2</sub> permeation and separation study at 100 kPa pressure difference and 30 °C for different membranes	137
4.12	Single gas fluxes of (a) CO <sub>2</sub> , (b) N <sub>2</sub> , (c) H <sub>2</sub> and (d) CH <sub>4</sub> through Ba-MW-2 membrane as a function of pressure difference for different temperature	145
4.13	Single gas permeances of (a) CO <sub>2</sub> , H <sub>2</sub> , and (b) N <sub>2</sub> , CH <sub>4</sub> through Ba-MW-2 membrane as a function of pressure difference at 30 °C	148
4.14	Single gas fluxes of (a) CO <sub>2</sub> , H <sub>2</sub> , and (b) N <sub>2</sub> , CH <sub>4</sub> through Ba-MW-2 membrane as a function of temperature at 100 kPa pressure difference across the membrane	150
4.15	Ideal selectivities of (a) CO <sub>2</sub> /CH <sub>4</sub> , (b) CO <sub>2</sub> /N <sub>2</sub> and (c) CO <sub>2</sub> /H <sub>2</sub> through Ba-MW-2 membrane as a function of pressure difference for different temperature	152
4.16	(a) Gas fluxes and (b) gas permeances through Ba-MW-2 membrane as a function of pressure difference for equimolar CO <sub>2</sub> /CH <sub>4</sub> gas mixture at 30 °C	154
4.17	CO <sub>2</sub> /CH <sub>4</sub> flux ratio and separation selectivity through Ba-MW-2 membrane as a function of pressure difference for equimolar CO <sub>2</sub> /CH <sub>4</sub> gas mixture at 30 °C	156
4.18	(a) Gas fluxes and (b) gas permeances through Ba-MW-2 membrane as a function of temperature for equimolar CO <sub>2</sub> /CH <sub>4</sub> gas mixture at 100 kPa pressure difference	157

4.19	CO <sub>2</sub> /CH <sub>4</sub> flux ratio and separation selectivity through Ba-MW-2 membrane as a function of temperature for equimolar CO <sub>2</sub> /CH <sub>4</sub> gas mixture at 100 kPa pressure difference	158
4.20	(a) Gas fluxes and (b) gas permeances through Ba-MW-2 membrane as a function of CO <sub>2</sub> concentration in the feed for CO <sub>2</sub> /CH <sub>4</sub> gas mixture at 100 kPa pressure difference and 30 °C	160
4.21	CO <sub>2</sub> /CH <sub>4</sub> flux ratio and separation selectivity through Ba-MW-2 membrane as a function of CO <sub>2</sub> concentration in the feed for CO <sub>2</sub> /CH <sub>4</sub> gas mixture at 100 kPa pressure difference and 30 °C	161
4.22	(a) Gas fluxes and (b) gas permeances through Ba-MW-2 membrane as a function of pressure difference for equimolar CO <sub>2</sub> /N <sub>2</sub> gas mixture at 30 °C	162
4.23	CO <sub>2</sub> /N <sub>2</sub> flux ratio and separation selectivity through Ba-MW-2 membrane as a function of pressure difference for equimolar CO <sub>2</sub> /N <sub>2</sub> gas mixture at 30 °C	164
4.24	(a) Gas fluxes and (b) gas permeances through Ba-MW-2 membrane as a function of temperature for equimolar CO <sub>2</sub> /N <sub>2</sub> gas mixture at 100 kPa pressure difference	165
4.25	CO <sub>2</sub> /N <sub>2</sub> flux ratio and separation selectivity through Ba-MW-2 membrane as a function of temperature for equimolar CO <sub>2</sub> /N <sub>2</sub> gas mixture at 100 kPa pressure difference	166
4.26	(a) Gas fluxes and (b) gas permeances through Ba-MW-2 membrane as a function of CO <sub>2</sub> concentration in the feed for CO <sub>2</sub> /N <sub>2</sub> gas mixture at 100 kPa pressure difference and 30 °C	167
4.27	CO <sub>2</sub> /N <sub>2</sub> flux ratio and separation selectivity through Ba-MW-2 membrane as a function of CO <sub>2</sub> concentration in the feed for CO <sub>2</sub> /N <sub>2</sub> gas mixture at 100 kPa pressure difference and 30 °C	169
4.28	(a) Gas fluxes and (b) gas permeances through Ba-MW-2 membrane as a function of pressure difference for equimolar CO <sub>2</sub> /H <sub>2</sub> gas mixture at 30 °C	170
4.29	CO <sub>2</sub> /H <sub>2</sub> flux ratio and separation selectivity through Ba-MW-2 membrane as a function of pressure difference for equimolar CO <sub>2</sub> /H <sub>2</sub> gas mixture at 30 °C	172
4.30	(a) Gas fluxes and (b) gas permeances through Ba-MW-2 membrane as a function of temperature for equimolar CO <sub>2</sub> /H <sub>2</sub> gas mixture at 100 kPa pressure difference	173
4.31	CO <sub>2</sub> /H <sub>2</sub> flux ratio and separation selectivity through Ba-MW-2 membrane as a function of temperature for equimolar CO <sub>2</sub> /H <sub>2</sub> gas mixture at 100 kPa pressure difference	174

4.32	(a) Gas fluxes and (b) gas permeances through Ba-MW-2 membrane as a function of CO <sub>2</sub> concentration in the feed for CO <sub>2</sub> /H <sub>2</sub> gas mixture at 100 kPa pressure difference and 30 °C	175
4.33	CO <sub>2</sub> /H <sub>2</sub> flux ratio and separation selectivity through Ba-MW-2 membrane as a function of CO <sub>2</sub> concentration in the feed for CO <sub>2</sub> /H <sub>2</sub> gas mixture at 100 kPa pressure difference and 30 °C	177
4.34	Durability test for gas permeation and separation of equimolar CO <sub>2</sub> /CH <sub>4</sub> gas mixture through Ba-MW-2 membrane at 100 kPa pressure difference and 30 °C	178
4.35	Durability test for gas permeation and separation of equimolar CO <sub>2</sub> /N <sub>2</sub> gas mixture through Ba-MW-2 membrane at 100 kPa pressure difference and 30 °C	178
4.36	Durability test for gas permeation and separation of equimolar CO <sub>2</sub> /H <sub>2</sub> gas mixture through Ba-MW-2 membrane at 100 kPa pressure difference and 30 °C	179
4.37	Effect of pressure difference and temperature on 1/(CO <sub>2</sub> permeance) at 27.5 % CO <sub>2</sub> in the feed	192
4.38	Effect of pressure difference and CO <sub>2</sub> % in the feed on 1/(CO <sub>2</sub> permeance) at temperature of 105 °C	192
4.39	Effect of temperature and CO <sub>2</sub> % in the feed on 1/(CO <sub>2</sub> permeance) at pressure difference of 300 kPa	193
4.40	Effect of pressure difference and temperature on 1/(CO <sub>2</sub> /CH <sub>4</sub> separation selectivity) at 27.5 % CO <sub>2</sub> in the feed	195
4.41	Effect of pressure difference and CO <sub>2</sub> % in the feed on 1/(CO <sub>2</sub> /CH <sub>4</sub> separation selectivity) at temperature of 105 °C	195
4.42	Effect of temperature and CO <sub>2</sub> % in the feed on 1/(CO <sub>2</sub> /CH <sub>4</sub> separation selectivity) at pressure difference of 300 kPa	196
4.43	Effect of pressure difference and temperature on 1/(CO <sub>2</sub> permeance) at 27.5 % CO <sub>2</sub> in the feed	202
4.44	Effect of pressure difference and CO <sub>2</sub> % in the feed on 1/(CO <sub>2</sub> permeance) at temperature of 105 °C	202
4.45	Effect of temperature and CO <sub>2</sub> % in the feed on 1/(CO <sub>2</sub> permeance) at pressure difference of 300 kPa	203
4.46	Effect of pressure difference and temperature on 1/(CO <sub>2</sub> /N <sub>2</sub> separation selectivity) at 27.5 % CO <sub>2</sub> in the feed	205
4.47	Effect of pressure difference and CO <sub>2</sub> % in the feed on 1/(CO <sub>2</sub> /N <sub>2</sub> separation selectivity) at temperature of 105 °C	205

4.48	Effect of temperature and CO <sub>2</sub> % in the feed on 1/(CO <sub>2</sub> /N <sub>2</sub> separation selectivity) at pressure difference of 300 kPa	206
4.49	Effect of pressure difference and temperature on 1/(CO <sub>2</sub> permeance) at 27.5 % CO <sub>2</sub> in the feed	212
4.50	Effect of pressure difference and CO <sub>2</sub> % in the feed on 1/(CO <sub>2</sub> permeance) at temperature of 105 °C	212
4.51	Effect of temperature and CO <sub>2</sub> % in the feed on 1/(CO <sub>2</sub> permeance) at pressure difference of 300 kPa	213
4.52	Effect of pressure difference and temperature on 1/(CO <sub>2</sub> /H <sub>2</sub> separation selectivity) at 27.5 % CO <sub>2</sub> in the feed	215
4.53	Effect of pressure difference and CO <sub>2</sub> % in the feed on 1/(CO <sub>2</sub> /H <sub>2</sub> separation selectivity) at temperature of 105 °C	215
4.54	Effect of temperature and CO <sub>2</sub> % in the feed on 1/(CO <sub>2</sub> /H <sub>2</sub> separation selectivity) at pressure difference of 300 kPa	216
4.55	Simulated and experimental single gas fluxes of CO <sub>2</sub> through Ba-MW-2 membrane at pressure difference of (a) 100 kPa, (b) 200 kPa, (c) 300 kPa, (d) 400 kPa and (e) 500 kPa. The empty markers connected by dashed lines and the solid markers are respectively simulated and experimental results	225
4.56	Simulated and experimental single gas fluxes of CH <sub>4</sub> through Ba-MW-2 membrane at pressure difference of (a) 100 kPa, (b) 200 kPa, (c) 300 kPa, (d) 400 kPa and (e) 500 kPa. The empty markers connected by dashed lines and the solid markers are respectively simulated and experimental results	226
4.57	Simulated and experimental single gas fluxes of N <sub>2</sub> through Ba-MW-2 membrane at pressure difference of (a) 100 kPa, (b) 200 kPa, (c) 300 kPa, (d) 400 kPa and (e) 500 kPa. The empty markers connected by dashed lines and the solid markers are respectively simulated and experimental results	226
4.58	Simulated and experimental single gas fluxes of H <sub>2</sub> through Ba-MW-2 membrane at pressure difference of (a) 100 kPa, (b) 200 kPa, (c) 300 kPa, (d) 400 kPa and (e) 500 kPa. The empty markers connected by dashed lines and the solid markers are respectively simulated and experimental results	227
4.59	Simulated and experimental CO <sub>2</sub> /CH <sub>4</sub> ideal selectivities through Ba-MW-2 membrane at pressure difference of (a) 100 kPa, (b) 200 kPa, (c) 300 kPa, (d) 400 kPa and (e) 500 kPa. The empty markers connected by dashed lines and the solid markers are respectively simulated and experimental results	228

4.60	Simulated and experimental CO <sub>2</sub> /N <sub>2</sub> ideal selectivities through Ba-MW-2 membrane at pressure difference of (a) 100 kPa, (b) 200 kPa, (c) 300 kPa, (d) 400 kPa and (e) 500 kPa. The empty markers connected by dashed lines and the solid markers are respectively simulated and experimental results	229
4.61	Simulated and experimental CO <sub>2</sub> /H <sub>2</sub> ideal selectivities through Ba-MW-2 membrane at pressure difference of (a) 100 kPa, (b) 200 kPa, (c) 300 kPa, (d) 400 kPa and (e) 500 kPa. The empty markers connected by dashed lines and the solid markers are respectively simulated and experimental results	230
4.62	Experimental and simulated result of (a) gas fluxes and (b) gas permeances for equimolar CO <sub>2</sub> /CH <sub>4</sub> gas mixture through Ba-MW-2 membrane at 100 kPa pressure difference. The experimental results are represented by solid markers and the simulated results are represented by lines connecting marker <sup>x</sup> or <sup>+</sup>	232
4.63	Experimental and simulated result of separation selectivities for equimolar CO <sub>2</sub> /CH <sub>4</sub> gas mixture through Ba-MW-2 membrane at 100 kPa pressure difference. The experimental results are represented by solid markers and the simulated results are represented by lines connecting marker <sup>x</sup>	233
4.64	Experimental and simulated result of (a) gas fluxes and (b) gas permeances for equimolar CO <sub>2</sub> /N <sub>2</sub> gas mixture through Ba-MW-2 membrane at 100 kPa pressure difference. The experimental results are represented by solid markers and the simulated results are represented by lines connecting marker <sup>x</sup> or <sup>+</sup>	234
4.65	Experimental and simulated result of separation selectivities for equimolar CO <sub>2</sub> /N <sub>2</sub> gas mixture through Ba-MW-2 membrane at 100 kPa pressure difference. The experimental results are represented by solid markers and the simulated results are represented by lines connecting marker <sup>x</sup>	235
4.66	Experimental and simulated result of (a) gas fluxes and (b) gas permeances for equimolar CO <sub>2</sub> /H <sub>2</sub> gas mixture through Ba-MW-2 membrane at 100 kPa pressure difference. The experimental results are represented by solid markers and the simulated results are represented by lines connecting marker <sup>x</sup> or <sup>+</sup>	236
4.67	Experimental and simulated result of separation selectivities for equimolar CO <sub>2</sub> /H <sub>2</sub> gas mixture through Ba-MW-2 membrane at 100 kPa pressure difference. The experimental results are represented by solid markers and the simulated results are represented by lines connecting marker <sup>x</sup>	237
4.68	Comparison between simulated and experimental single gas fluxes through Ba-MW-2 membrane at temperature of 40, 80, 120, 160 °C and 150 kPa pressure difference	238

4.69	Comparison between simulated and experimental ideal selectivities for single gas permeation through Ba-MW-2 membrane at temperature of 40, 80, 120, 160 °C and 150 kPa pressure difference	239
4.70	Comparison between simulated and experimental results for permeation and separation of equimolar CO <sub>2</sub> /CH <sub>4</sub> gas mixture through Ba-MW-2 membrane at temperature of 40, 80, 120, 160 °C and 100 kPa pressure difference	241
4.71	Comparison between simulated and experimental results for permeation and separation of equimolar CO <sub>2</sub> /N <sub>2</sub> gas mixture through Ba-MW-2 membrane at temperature of 40, 80, 120, 160 °C and 100 kPa pressure difference	242
4.72	Comparison between simulated and experimental results for permeation and separation of equimolar CO <sub>2</sub> /H <sub>2</sub> gas mixture through Ba-MW-2 membrane at temperature of 40, 80, 120, 160 °C and 100 kPa pressure difference	243
A.1.1	Schematic of the heating mechanism of (a) direct in-situ crystallization and (b) MW heating	269
A.1.2	Pore size distribution of (a) HS-24 and (b) MW-2 zeolite powder samples	270
B.2.1	Chromatogram of equimolar CO <sub>2</sub> /CH <sub>4</sub> gas mixture	273
B.2.2	Chromatogram of equimolar CO <sub>2</sub> /N <sub>2</sub> gas mixture	274
B.2.3	Chromatogram of equimolar CO <sub>2</sub> /H <sub>2</sub> gas mixture	274
C.1.1	Plot of single gas fluxes versus $\ln\left(\frac{1 + b_i p_{feed}}{1 + b_i p_{perm}}\right)$ for (a) CO <sub>2</sub> , (b) CH <sub>4</sub> , (c) N <sub>2</sub> and (d) H <sub>2</sub> . The solid lines are the best straight lines to fit all the data	280
C.1.2	Plot of ln(adsorption equilibrium constant) versus inverse temperature for (a) CO <sub>2</sub> , CH <sub>4</sub> and (b) N <sub>2</sub> , H <sub>2</sub> adsorption on Ba-MW-2 membrane. The solid lines are the best straight lines to fit all the data	281
C.1.3	Plot of ln(M-S diffusivity) versus inverse temperature for (a) CO <sub>2</sub> , (b) CH <sub>4</sub> , (c) N <sub>2</sub> and (d) H <sub>2</sub> on Ba-MW-2 membrane. The solid lines are the best straight lines to fit all the data	283

## LIST OF PLATES

	Page
3.1 Photograph of stainless steel reactor for direct in-situ crystallization of the zeolite membranes	72
3.2 Photograph of MW reactor for MW heating of the zeolite membranes	73
3.3 Photograph of reflux system for modification (ion-exchange) of the zeolite membranes	78
3.4 Photograph of gas permeation and separation test rig with GC	86
3.5 Photograph of gas permeation cell	90
4.1 SEM images of top view of (a) HS-24, (b) MW-0.5, (c) MW-1, (d) MW-2 and (e) MW-3 membranes	108
4.2 SEM images of cross section view of (a) HS-24, (b) MW-0.5, (c) MW-1, (d) MW-2 and (e) MW-3 membranes	112
4.3 TEM images of (a) HS-24 and (b) MW-2 zeolite powder samples	120
4.4 HRTEM images of pore channel of (a) HS-24 and (b) MW-2 zeolite powder samples	121
4.5 SAED micrographs of (a) HS-24 and (b) MW-2 zeolite powder samples	122

## LIST OF ABBREVIATIONS

<b>Symbol</b>	<b>Description</b>
AFI	Aluminophosphate – five (AlPO <sub>4</sub> -5)
$\alpha$ -Al <sub>2</sub> O <sub>3</sub>	alfa-alumina
Al(i-C <sub>3</sub> H <sub>7</sub> O) <sub>3</sub>	Aluminium isopropoxide
ANOVA	Analysis of variance
Ar	Argon
ATN	MgAlPO <sub>4</sub> - thirty-nine (MAPO-39)
ATR	Attenuated Total Reflectance
Ba <sup>2+</sup>	Barium cation
BEA	Zeolite Beta
BET	Brunauer-Emmett-Teller
BJH	Barrett-Joyner-Halenda
BPR	Back pressure regulator
Ca <sup>2+</sup>	Calcium cation
CCD	Central composite design
CHA	Chabazite
CH <sub>4</sub>	Methane
CMS	Carbon molecular sieve
CO <sub>2</sub>	Carbon dioxide
CV	Check valve
DDR	Decadodecasil-3R
DI	Deionized
DOE	Design of experiment
EDI	Edingtonite
EDS	Energy Dispersive Spectroscopy
FAU	Faujasite

FCOM	Fluorescent confocal optical microscopy
FER	Zeolite Socony Mobil – thirty five (ZSM-35)
FTIR	Fourier Transformed Infra Red
FTM	Facilitated transport membrane
GC	Gas chromatography
H <sub>2</sub>	Hydrogen
H <sub>3</sub> PO <sub>4</sub>	Phosphoric acid
HK	Horvath-Kawazoe
ITV	Instituto de Tecnologia Quimica Valencia – thirty seven (ITQ-37)
IZA-SC	International Zeolite Association Structure Commission
IRR	Instituto de Tecnologia Quimica Valencia – fourty four (ITQ-44)
IZA	International Zeolite Association
LTA	Linde A
MDES	Methyldiethoxysilane
MEA	Monoethanolamine
MEL	Zeolite Socony Mobil – eleven (ZSM-11)
MFI	Zeolite Socony Mobil – five (ZSM-5)
MLD	Molecular layer deposition
MMM	Mixed matrix membrane
Mg <sup>2+</sup>	Magnesium cation
MOF	Metal-organic framework
MOR	Mordenite
M-S	Maxwell-Stefan
MW	Microwave
N <sub>2</sub>	Nitrogen
NV	Needle valve
OFF	Offertite

PEEK	PolyEtherEtherKetone
PG	Pressure gauge
“Prob > F”	Probability
RTP	Rapid thermal processing
SAED	Selected area electron diffraction
SAPO-5	Silicoaluminophosphate – five
SAPO-34	Silicoaluminophosphate – thirty four
SDA	Structure directing agent
SEM	Scanning Electron Microscopy
SOD	Sodalite
Sr <sup>2+</sup>	Strontium cation
TEAOH	Tetraethylammonium hydroxide
TEM	Transmission Electron Microscope
TGA	Thermal Gravimetric Analysis
TSA	Temperature swing adsorption
TWV	Three way valve
UWY	Institut Français du Pétrole and University of Mulhouse – twenty (IM-20)
VPT	Vapor phase transport
VSA	Vacuum and pressure swing adsorption
XRD	X-ray diffraction

## LIST OF SYMBOLS

Symbol	Description	Unit
A	Factor code of temperature in DOE	-
$A_m$	Effective area of the zeolite membrane	$m^2$
B	Factor code of pressure difference in DOE	-
$b$	Adsorption equilibrium constant	$kPa^{-1}$
C	Factor code of CO <sub>2</sub> % in the feed in DOE	-
$D_{ms}$	Maxwell-Stefan diffusivity	$m^2/s$
$D_{ms0}$	Infinite Maxwell-Stefan diffusivity	$m^2/s$
$d, e, f$	The lengths of crystallographic axes in different directions of a unit cell	Å
$\Delta H$	Heat of adsorption	$kJ/mol$
$\Delta S$	Entropy of adsorption	$J/mol.K$
$E$	Activation energy of Maxwell-Stefan diffusivity	$J/mol$
$F_i$	Gas flow of component $i$ .	$mol/s$
M	Molecular weight	$g/mol$
$N_i$	Gas flux of component $i$	$mol/m^2.s$
$n$	Number of process variables in the model equation generated by DOE	-
$p$	Pressure	Pa
$P_i$	Gas permeance of component $i$	$mol/m^2.s$ .Pa
$\Delta p_i$	Partial pressure difference of component $i$ across the membrane	Pa
$q_i$	Molar loading of component $i$	$mol/kg$
$R$	Gas constant	$J/mol.K$
$R^2$	Regression coefficient	-

$T$	Temperature	°C or K
$t$	Time	s or min
$x_v$ and $x_w$	Process variables in the model equation generated by DOE	-
$x_v x_w$	First order interaction between $x_v$ and $x_w$ in the model equation generated by DOE	-
$y$	Response in the model equation generated by DOE	-
$z$	Distance from feed side of membrane	m

*Greek Letters*

$\varphi_0$	Regression coefficient for intercept terms in the model equation generated by DOE	-
$\varphi_v$	Regression coefficient for linear terms in the model equation generated by DOE	-
$\varphi_{vv}$	Regression coefficient for quadratic terms in the model equation generated by DOE	-
$\varphi_{vw}$	Regression coefficient for interaction terms in the model equation generated by DOE	-
$\varepsilon, \beta, \gamma$	The angles between the crystallographic axes of a unit cell	°
$\alpha_{i/j}$	Selectivity of component $i$ over component $j$	-
$\zeta$	Error in the model equation generated by DOE	-
$\delta_{ij}$	Kronecker delta	-
$\delta_m$	The thickness of the membrane	m
$\theta_i$	Fractional coverage of component $i$	-
$\rho$	Density of the membrane	kg/m <sup>3</sup>
$(\nabla\mu_i)$	Chemical potential gradient causing driving force for diffusion	J/mol
$\Gamma_i$	Thermodynamic correction factor of component $i$	-

*Subscripts*

<i>feed</i>	Feed stream	-
<i>i, j</i>	Component gas CO <sub>2</sub> , N <sub>2</sub> , CH <sub>4</sub> or H <sub>2</sub>	-
<i>perm</i>	Permeate stream	-
<i>ret</i>	Retentate stream	-

*Superscripts*

<i>ideal</i>	Ideal	-
<i>s</i>	Single gas	-
<i>sat</i>	Saturated	-
<i>sep</i>	Separation	-

**SINTESIS, PENCIRIAN DAN PENGUBAHSUAIAN MEMBRAN ZEOLIT  
SAPO-34 UNTUK PEMISAHAN CO<sub>2</sub> DARIPADA CAMPURAN-  
CAMPURAN GAS PERDUAAN**

**ABSTRAK**

Dalam kajian ini, membran zeolit silikoauminofosfat – tiga puluh empat (SAPO-34) disintesis di atas penyokong  $\alpha$ -alumina berbentuk cakera dengan menggunakan (1) penghabluran in-situ terus dan (2) pemanasan gelombang mikro (MW). Pemanasan MW membentuk membran SAPO-34 yang lebih nipis (ketebalan  $\sim 1.6 \mu\text{m}$ ) dengan taburan saiz kristal zeolit ( $\sim 0.6 \mu\text{m}$ ) yang lebih kecil dalam masa sintesis sebanyak 2 jam pada  $200\text{ }^\circ\text{C}$ , yang lebih pendek daripada penghabluran in-situ terus. Membran SAPO-34 yang disintesis dengan menggunakan pemanasan MW telah diubahsuai dengan proses pertukaran ion dengan menggunakan kation  $\text{Mg}^{2+}$ ,  $\text{Ca}^{2+}$ ,  $\text{Sr}^{2+}$  dan  $\text{Ba}^{2+}$ . Sifat-sifat membran tersebut dicirikan dengan TEM, XRD, SEM, TGA, EDS, FT-IR dan penyerapan-penyahjerapan nitrogen. Membran zeolit SAPO-34 yang diubahsuai dengan  $\text{Ba}^{2+}$  meningkatkan kememilihan pemisahan  $\text{CO}_2/\text{CH}_4$ ,  $\text{CO}_2/\text{N}_2$  dan  $\text{CO}_2/\text{H}_2$  masing-masing sebanyak 240, 217 dan 127 % dalam kajian penelapan dan pemisahan campuran gas sama molal. Membran zeolit SAPO-34 yang diubahsuai dengan  $\text{Ba}^{2+}$  diuji untuk penelapan satu gas  $\text{CO}_2$ ,  $\text{CH}_4$ ,  $\text{N}_2$  dan  $\text{H}_2$ . Penelapan dan pemisahan gas perduaan  $\text{CO}_2/\text{CH}_4$ ,  $\text{CO}_2/\text{N}_2$  dan  $\text{CO}_2/\text{H}_2$  juga dikaji. Kaedah permukaan gerak balas (RSM) digunakan untuk mengoptimumkan parameter proses untuk penelapan dan pemisahan gas perduaan  $\text{CO}_2/\text{CH}_4$ ,  $\text{CO}_2/\text{N}_2$  dan  $\text{CO}_2/\text{H}_2$ . Model matematik yang dibangunkan berdasarkan gabungan pendekatan perumusan Maxwell-Stefan dan garis sesuhu Langmuir, dapat mewakili penelapan satu gas, penelapan dan pemisahan gas perduaan dari segi telapan dan kememilihan pemisahan bagi gas melalui membran SAPO-34 yang diubahsuai dengan  $\text{Ba}^{2+}$  dengan ralat  $\pm 10\%$ .

# SYNTHESIS, CHARACTERIZATION AND MODIFICATION OF SAPO-34 ZEOLITE MEMBRANE FOR SEPARATION OF CO<sub>2</sub> FROM BINARY GAS MIXTURES

## ABSTRACT

In the present research, silicoaluminophosphate – thirty four (SAPO-34) zeolite membranes were synthesized on  $\alpha$ -alumina disc support using (1) direct in-situ crystallization and (2) microwave (MW) heating. MW heating formed thinner SAPO-34 membrane (thickness of  $\sim 1.6 \mu\text{m}$ ) with narrower zeolite crystal size distribution ( $\sim 0.6 \mu\text{m}$ ) in much shortened synthesis time of 2 hours at 200 °C compared to direct in-situ crystallization. The SAPO-34 membranes synthesized using MW heating were modified by ion-exchange process with Mg<sup>2+</sup>, Ca<sup>2+</sup>, Sr<sup>2+</sup> and Ba<sup>2+</sup> cations. The membranes were characterized using TEM, XRD, SEM, TGA, EDS, FT-IR and nitrogen adsorption-desorption. The Ba<sup>2+</sup>-modified SAPO-34 zeolite membrane increased the CO<sub>2</sub>/CH<sub>4</sub>, CO<sub>2</sub>/N<sub>2</sub> and CO<sub>2</sub>/H<sub>2</sub> separation selectivity by 240, 217 and 127 % respectively in the equimolar gas mixture permeation and separation. The Ba<sup>2+</sup>-modified SAPO-34 zeolite membrane was tested for single gas permeation of CO<sub>2</sub>, CH<sub>4</sub>, N<sub>2</sub>, H<sub>2</sub>. The binary gas permeation and separation of CO<sub>2</sub>/CH<sub>4</sub>, CO<sub>2</sub>/N<sub>2</sub> and CO<sub>2</sub>/H<sub>2</sub> was also studied. Response surface methodology (RSM) were used to optimize the process parameters for binary gas permeation and separation of CO<sub>2</sub>/CH<sub>4</sub>, CO<sub>2</sub>/N<sub>2</sub> and CO<sub>2</sub>/H<sub>2</sub>. Mathematical models, developed based on combined approaches of Maxwell-Stefan formulation and Langmuir isotherm, were able to predict the single gas permeation, binary gas permeation and separation (in terms of permeance and selectivity) through the Ba<sup>2+</sup>-modified SAPO-34 membrane within an error of  $\pm 10 \%$ .

# CHAPTER 1

## INTRODUCTION

### 1.1 Zeolite

Zeolites are crystalline silicates or aluminosilicates, based on a three-dimensional arrangement of  $TO_4$  tetrahedral ( $SiO_4$  or  $AlO_4$ ), where T is silicon (Si) or aluminium (Al) atom, connected through their oxygen atoms to form subunits and finally large lattices by repeating identical building blocks (unit cells). The structural formula of zeolite is  $M_{x/n}(AlO_2)_x(SiO_2)_y$  where n is the valence of cation M, x + y the total number of tetrahedral per unit cell and y/x the atomic Si/Al ratio varying from a minimal value of 1 to infinite (Guisnet and Gilson, 2002).

Most of the zeolites can be classified into three categories (Guisnet and Gilson, 2002):

- Small pore zeolites with 8 membered-ring pore apertures (8 tetrahedral atoms and 8 oxygen atoms) having free diameters of 0.30 – 0.45 nm.
- Medium pore zeolites with 10 membered-ring apertures having free diameters of 0.45 – 0.60 nm.
- Large pore zeolites with 12 membered-ring apertures having free diameters of 0.60 – 0.80 nm.

Each framework structure of zeolites were identified by the International Zeolite Association Structure Commission (IZA-SC) using a code consisting three capital letters. More than 130 zeolite framework structures have been listed by the Atlas of Framework Types in year 2011 (Baerlocher *et al.*, 2001). Table 1.1 presents

the examples of zeolite with their framework structure' codes reported in the literature. Those framework structures include Aluminophosphate – five (AFI), MgAlPO<sub>4</sub> - thirty-nine (ATN), Zeolite Beta (BEA), Chabazite (CHA), Decadodecasil-3R (DDR), Edingtonite (EDI), Faujasite (FAU), Zeolite Socony Mobil – thirty five (FER), Instituto de Tecnologia Quimica Valencia – thirty seven (ITV), Instituto de Tecnologia Quimica Valencia – forty four (IRR), Linde A (LTA), Zeolite Socony Mobil – eleven (MEL), Zeolite Socony Mobil – five (MFI), Mordenite (MOR) < Offertite (OFF), Sodalite (SOD) and Institut Français du Pétrole and University of Mulhouse (UWY).

**Table 1.1:** Different zeolite framework structures reported in the literature (Bowen *et al.*, 2004; Julbe, 2007; Payra and Dutta, 2003)

Framework Structure	Corresponding Zeolite	Pore size (nm)
SOD	Sodalite	0.28
EDI	Edingtonite	0.28 x 0.38 and 0.8
CHA	SSZ-13, SAPO-34	0.38
ATN	MAPO-39	0.4
LTA	NaA	0.41
DDR	Decadodecasil	0.36 x 0.44
OFF-FER Intergrowth	T-type	0.36 x 0.51
MEL	ZSM-11	0.53 x 0.54
FER	ZSM-35	0.42 x 0.54 and 0.35 x 0.48
MFI	Silicalite-1, ZSM-5	0.53 x 0.56 and 0.51 x 0.55
OFF	Offertite	0.67 and 0.36 x 0.49
MOR	Mordenite	0.67 x 0.70 and 0.26 x 0.57
AFI	AlPO <sub>4</sub> -5	0.73
FAU	NaX, NaY	0.74
BEA	Beta	0.73 x 0.60

Each framework structure displays distinctive pore structure and pore size. So far, the MFI framework structure is the most common zeolite used for various applications such as in catalysis and membrane separation. The MFI structure includes Silicalite-1 (pure silica zeolite) and ZSM-5 (alumino-silicate zeolite)

(Bowen *et al.*, 2004). Lately, three new zeolite framework structures have been approved by the IZA Structure Commission in the year of 2011 and these zeolites are classified as Instituto de Tecnologia Quimica Valencia – thirty seven (ITV), Instituto de Tecnologia Quimica Valencia – forty four (IRR) and Institut Français du Pétrole and University of Mulhouse – twenty (UWY) (IZA-SC, 2011).

## **1.2 Zeolite Membrane**

Generally, zeolite materials are prepared in the form of fine particles and agglomerate with desired shapes and sizes. The zeolite micropores in molecular size enable them to be used widely in applications such as adsorption, catalysis and ion exchange (Coronas, 2010). However, the zeolite materials in bulk form are not efficient for some applications and the preparation of zeolite materials as a thin layer is needed (Valtchev and Mintova, 2001). Zeolite membranes, are getting increasing importance in number of emerging applications such as chemical sensors, insulating layers in microprocessors, ion exchange electrodes, corrosion protection coatings, catalytic membrane reactor and membrane separator (Snyder and Tsapatsis, 2007; Choi *et al.*, 2009).

Zeolite membranes are generally formed by depositing zeolite layers on porous supports. Figure 1.1 shows the schematic of a supported zeolite membrane. The zeolite membrane acts as a selective barrier between two phases of fluid (Ismail *et al.*, 2002). When the fluid is fed to the supported zeolite membrane, the phase that passes through the zeolite membrane is called permeate while retentate is the phase that is unable to pass through the zeolite membrane.

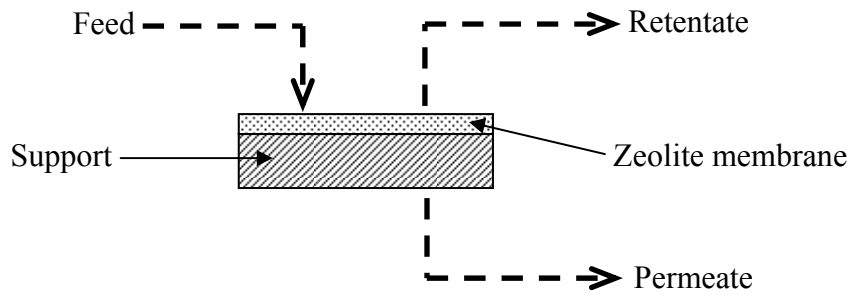


**Figure 1.1:** Schematic of a supported zeolite membrane

### 1.3 Gas Separation

#### 1.3.1 Issue of CO<sub>2</sub> Gas Separation

The emission of carbon dioxide (CO<sub>2</sub>) contributed to 80 % of current greenhouse gas emission to the atmosphere (Nair *et al.*, 2009). The increasing CO<sub>2</sub> concentration in the atmosphere in recent years and its implication on global warming has drawn attention of many researchers around the globe, creating the need for extensive investigation of CO<sub>2</sub> capture and separation (Li *et al.*, 2011a). Separation and recovery of CO<sub>2</sub> from large emission sources remained a great challenge nowadays in restricting the emission of greenhouse gas into the atmosphere. The CO<sub>2</sub> separation from methane (CH<sub>4</sub>), nitrogen (N<sub>2</sub>) and hydrogen (H<sub>2</sub>) from the natural gas streams, power plant flue gas streams and fuel gas streams (i.e. in water-gas shift reaction) respectively, are among the main concerns nowadays for carbon dioxide removal and recovery to minimize its effect on the environment in terms of green house gases effect. CO<sub>2</sub> removal from these gas streams is also essential in the production of pure CH<sub>4</sub>, N<sub>2</sub> and H<sub>2</sub> as industrially important energy and chemical sources. In view of this issue, there are increasing number of articles published by the researchers with the aim of finding potential processes for CO<sub>2</sub> capture, separation and CO<sub>2</sub> enrichment from exhaust gases to reduce carbon emissions directly at the source through greenhouse grown plant

uptake (Habib *et al.*, 2011; Scholes *et al.*, 2010; D'Alessandro *et al.*, 2010; Hasib-ur-Rahman *et al.*, 2010; Budd and McKeown, 2010; Mansourizadeh and Ismail, 2009; Krull *et al.*, 2008; Dion *et al.*, 2011; Jaffrin *et al.*, 2003).

### 1.3.2 Conventional Method for CO<sub>2</sub> Gas Separation

Figure 1.2 shows the common technologies available for separation of CO<sub>2</sub>. Conventional methods for CO<sub>2</sub> separation include cryogenic distillation, absorption and adsorption processes. Cryogenic distillation enables CO<sub>2</sub> separation from relatively high purity (> 90 %) sources on the basis of cooling and condensation. However, it is expensive and energy intensive due to its operation at very low temperature (lower than -73 °C for liquefaction of CO<sub>2</sub>) and at elevated pressure (Li *et al.*, 2011a; Olajire, 2010; Leo *et al.*, 2009).

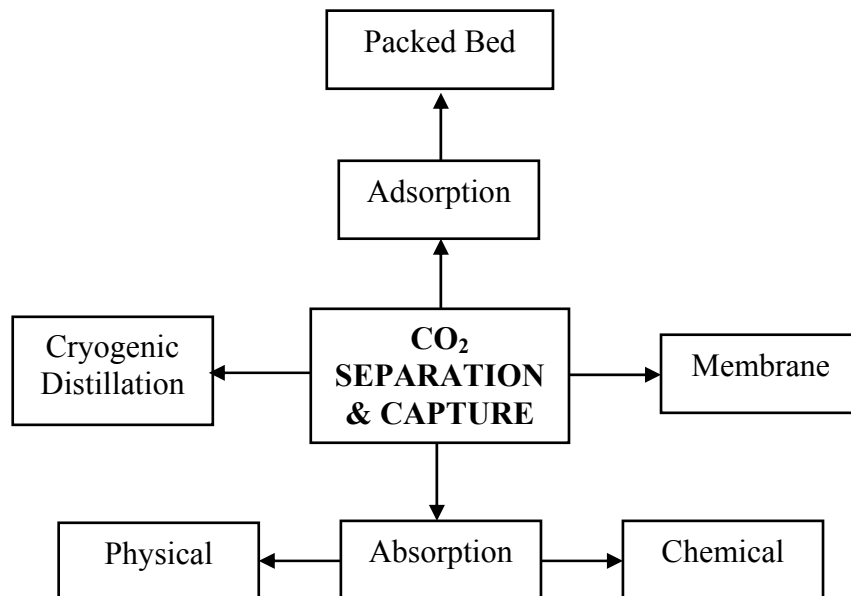


**Figure 1.2:** Common technologies for CO<sub>2</sub> separation (Li *et al.*, 2011a; Olajire, 2010)

Absorption, either chemical or physical, is another approach which is widely used for CO<sub>2</sub> separation. In chemical absorption, CO<sub>2</sub> is chemically captured through the acid-base neutralization reaction with caustic solvents such as

monoethanolamine (MEA) following by the driven-off of CO<sub>2</sub> by heating the aqueous solution containing amine-bound CO<sub>2</sub>. The regeneration process required in the chemical absorption process is energy intensive (Bara *et al.*, 2009). Physical absorption, is another category of absorption in which CO<sub>2</sub> is bound selectively to the solvents (Fluor process, Rectisol process, ionic liquid etc) at high partial pressure and low temperature. However, physical absorption brings about drawback such as high capital cost of Fluor and Rectisol plant. In addition, the high viscosity of ionic liquid results in limited mass transfer and hence low absorption rates (D'Alessandro *et al.*, 2010; Hasib-ur-Rahman *et al.*, 2010; Olajire, 2010).

Adsorption is another well established method for CO<sub>2</sub> separation. Common solid adsorbents used include metal oxides, carbons, zeolites, ion exchange resins, activated alumina and metal-organic framework (MOF). The CO<sub>2</sub> separation is achieved by CO<sub>2</sub> adsorption to the solid adsorbents through physisorption (van der Waals) or chemisorption (covalent bonding), and followed by regeneration of the CO<sub>2</sub>-adsorbed solid adsorbent through processes such as temperature swing adsorption (TSA), vacuum and pressure swing adsorption (VSA). The high power requirement for the adsorbent regeneration led to high capital cost of these processes (Li *et al.*, 2011a; D'Alessandro *et al.*, 2010).

### **1.3.3 Membrane-based CO<sub>2</sub> Gas Separation Technology**

Membrane-based separation technology has attracted great deal of research interest for CO<sub>2</sub> separation in views of the requirement for reduction in the environmental impact, operation cost, energy utilization and waste generation (Bernardo *et al.*, 2009). Membrane offers advantages such as high energy efficiency

and operational simplicity compared to conventional CO<sub>2</sub> separation units (Lin and Freeman, 2005). It is mechanical robust as it needs no moving part and hence can be used in remote locations (Ismail *et al.*, 2009). Membrane enables continuous separation of gas by filtering one or more gases from the feed mixture based on the differences in physical and/or chemical interplays between the membrane and the gases (Olajire, 2010). Membrane can be categorized into organic (polymeric) and inorganic. Inorganic membranes include ceramic, carbon, oxides and different types of zeolites.

Polymeric membranes, are widely used for the membrane gas separation due to its low energy cost, ease in fabrication and scalability (Ismail *et al.*, 2009; Basu *et al.*, 2010). However, the application of polymeric membranes is limited to its loss in performance stability at high temperature, high pressure and in the highly acidic or alkaline environment (Koros and Mahajan, 2000). In addition, polymeric membranes, specially the type of glassy polymers, encounter plasticization problem in the presence of CO<sub>2</sub> even in low concentration. The swelling of polymer matrix occurs during plasticization resulted in permanent enlargement of interchain spacing in the polymer matrix. The matrix damage leads to reduced CO<sub>2</sub> gas separation performance of polymeric membrane (Bernardo *et al.*, 2009; Basu *et al.*, 2010; Baker, 2002).

Inorganic membranes are gaining increasing interest among the researchers for separation of CO<sub>2</sub> in view of their higher thermal, chemical and mechanical stability compared to organic membranes (Ismail *et al.*, 2009; Botias *et al.*, 2010). The porous inorganic membranes available commercially include carbon, glass,

oxide and zeolite membranes. The pore size of these membranes vary from microporous to mesoporous (< 25 nm) for carbon, oxide, zeolite and from mesoporous to macroporous (> 1 nm) for glass materials (Phair and Badwal, 2006). Besides, these membranes also differ in properties such as surface area, thermal and chemical stability (Meinema *et al.*, 2005). Carbon molecular sieve (CMS) membranes, prepared from carbonization of polymer precursors, have been widely investigated for its gas separation ability. Despite higher production cost of CMS membranes, they offer advantages such as higher permeance and separation performance compared to polymeric membranes (Hagg and He, 2011). However, careful handling is essential for CMS membranes since they suffer from the problem of brittleness (Bernardo *et al.*, 2009; Adhikari and Fernando, 2006; Ismail and David, 2001; Salleh *et al.*, 2011).

The development of facilitated transport membranes (FTMs) and mixed matrix membranes (MMMs) is another trend that emerges in the membrane-based gas separation technology. FTMs are good candidates for CO<sub>2</sub> separation on the basis of selective CO<sub>2</sub> transport using a carrier molecule with affinity to CO<sub>2</sub>. Examples of FTMs are the immobilized liquids with facilitators such as amino species, polar polymers and ionic liquids, supported on polymeric or ceramic porous supports. However, FTMs face challenges with long-term stability and low tolerance in handling gas separation with high CO<sub>2</sub> partial pressure. The phenomenon of carrier saturation leads to decline in CO<sub>2</sub> separation performance of FTMs as the CO<sub>2</sub> partial pressure increases (Scholes *et al.*, 2010; Bernardo *et al.*, 2009). On the other hand, MMMs are formed by homogeneously incorporating the discrete phase (typically inorganic solids) in a continuous polymer phase. The combined strength

of two different phases, such as high selectivity of inorganic phase and low cost of polymer phase, makes MMMs attractive for CO<sub>2</sub> gas separation. However, MMMs encounter problems such as plasticization with CO<sub>2</sub> and easy formation of non-selective void spaces between polymer and inorganic phases (Li *et al.*, 2011a; Ismail *et al.*, 2009).

#### **1.3.4 Zeolite Membrane for CO<sub>2</sub> Gas Separation**

Zeolite membranes are the microporous inorganic membranes which are highly potential candidates for CO<sub>2</sub> gas separation. Besides possessing higher thermal, mechanical and chemical resistance compared to organic membranes, their well-defined, uniform and ordered molecular-sized pore structures make them attractive as shape-selective material for CO<sub>2</sub> gas separation (Shekhawat *et al.*, 2003; Sebastián *et al.*, 2007; Li *et al.*, 2006a; Jeong, 2010; Othman *et al.*, 2009). Choosing the suitable zeolite membrane with desired pore structure allows high gas separation performance by significantly discriminating the components in the gas stream on the basis of difference in molecular sieving, adsorption and diffusion effects (Caro *et al.*, 2000).

There have been extensive investigations on MFI and FAU zeolite membranes for the purpose of gas permeation and separation. MFI membrane with medium pore size (0.51-0.56 nm) and FAU membrane with large pore size (0.74 nm) enable satisfactory CO<sub>2</sub> separation performance. In recent years, the development of small-pore zeolite membrane (pore size < 0.45 nm) such as DDR and T-type, emerges as focus in research activities in exploring their ability in CO<sub>2</sub> gas separation. Silicoaluminophosphate – thirty four (SAPO-34), with CHA framework

structure consists of small pore structure. Figure 1.3 shows the framework structure of CHA. The SAPO-34 zeolite framework includes eight-ring apertures with an effective diameter of about 0.38 nm (Li *et al.*, 2004), which is close to the CO<sub>2</sub> gas molecule's kinetic diameter of 0.33 nm, make it potential candidate for CO<sub>2</sub> gas separation. Therefore, present study focused on synthesis of SAPO-34 zeolite membrane using novel method, modification of SAPO-34 zeolite membrane and its performance studies for CO<sub>2</sub> separation from CO<sub>2</sub>/CH<sub>4</sub>, CO<sub>2</sub>/N<sub>2</sub> and CO<sub>2</sub>/H<sub>2</sub> binary gas mixtures.

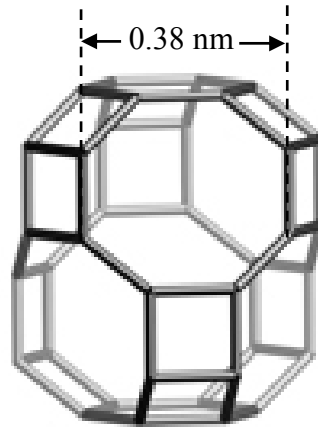


**Figure 1.3:** Framework structure of CHA (Li *et al.*, 2004; IZA-SC, 2008)

#### 1.4 Problem Statement

Preparation of uniform and thin zeolite membrane is a very challenging work. There are number of factors and its combined effect influences the quality of the membrane produced. The choice of the right preparation method, suitability of the synthesis condition and dust free clean environment are essential for formation of high quality zeolite membrane. Mostly zeolite membranes were synthesized through direct in-situ crystallization. The preparation method reported so far in the literature for the synthesis of SAPO-34 membranes is direct in-situ crystallization and secondary growth method. Owing to non-uniformity in SAPO-34 zeolite

crystals (sized 0.1-4  $\mu\text{m}$ ) synthesized through the syntheses reported in previous studies, the SAPO-34 membranes have been formed with thickness of 5-25  $\mu\text{m}$  (Li *et al.*, 2004; Poshusta *et al.*, 2000; Li *et al.*, 2005a; Li *et al.*, 2008). A good membrane should possess both high gas flux and separation selectivity for a gaseous component from the gaseous mixture. High gas flux is required for permeation and high separation selectivity is essential in confirming the high efficiency of the membrane separation system under low driving force, thus reducing the capital cost of the separation system (Lu *et al.*, 2007). However, membrane performance appears to be a tradeoff between gas flux and separation selectivity. The increase in the thickness of the membrane layer generally increases the gas separation selectivity, but at the same time it is attributed to the low flux of gaseous component. The preparation of a uniform and thin zeolite membrane with fewer defects, is desirable for both high gas flux and separation selectivity. This is one of the critical issues as well as a challenge to the researchers nowadays to synthesize the membrane with the desired properties and characteristics.

The direct in-situ crystallization for SAPO-34 zeolite membranes brings about a number of drawbacks and these include the requirement of long synthesis time in addition to the problem of formation of non-uniform SAPO-34 zeolite crystals. The development of zeolite membrane for gas separation is still a subject of intensive research in the laboratory scale nowadays due to its high capital cost. In addition, another challenging task is the reproducibility of the synthesis method for the formation of zeolite membrane with desired thickness. Therefore, alternative methodology for synthesis of zeolite membrane with much shortened time is required in order to reduce the capital cost. The method needs to be highly

reproducible and time-effective for the formation of SAPO-34 zeolite membrane with high quality (high gas flux and high separation selectivity). This will be the first step in the development of the zeolite membrane separation technology toward commercialization. In the present research, microwave (MW) heating appears to be potential technology for the synthesis of SAPO-34 zeolite membrane. The MW heating was reported to offer number of advantages such as rapid synthesis time of zeolite membrane and formation of zeolite crystals with higher uniformity compared to direct in-situ crystallization (Li and Yang, 2008).

Most of the CO<sub>2</sub> gas permeation and separation studies using zeolite membranes, including SAPO-34 zeolite membranes, were performed for equimolar binary gas mixtures which contains 50 % of CO<sub>2</sub> (Li *et al.*, 2004; Poshusta *et al.*, 2000; Li and Fan, 2010; Tian *et al.*, 2009; Hong *et al.*, 2008). Favre (2007) reported that in general the CO<sub>2</sub> concentration varies between 5-30 % in natural gas processing streams with mainly CH<sub>4</sub> gas and is 4-30 % in post combustion processing streams with mainly N<sub>2</sub>. As for the concern of separation of CO<sub>2</sub> from H<sub>2</sub>, the CO<sub>2</sub> concentration in the fuel gas streams (i.e. from steam reforming and gasification processes) may go as low as 4 % (Jeon *et al.*, 2008; Rajvanshi, 1986). The fuel gas compositions vary greatly depending on the process conditions and the feedstock compositions. This indicates that the CO<sub>2</sub> permeation and separation studies reported for SAPO-34 zeolite membranes so far did not reflect the real operation requirement in industrial separation systems. Therefore, it is highly desirable to study the performance of the SAPO-34 zeolite membranes for the separation of CO<sub>2</sub> from the feed gas mixtures with wide range of CO<sub>2</sub> concentration (as low as 5 %) in order to make the process more feasible for industrial application.

So far, high separation selectivities were achieved for gas mixtures CO<sub>2</sub>/CH<sub>4</sub> and CO<sub>2</sub>/N<sub>2</sub> using the reported SAPO-34 zeolite membranes. However, the SAPO-34 zeolite membranes showed very low separation selectivity, especially for gas mixture CO<sub>2</sub>/H<sub>2</sub> at high temperature. Hong *et al.* (2008) reported CO<sub>2</sub>/H<sub>2</sub> separation selectivity of more than 100 using SAPO-34 membrane at -20 °C. Such temperature was not applicable for the real industrial separation systems which are operated at temperature higher than room temperature. The SAPO-34 membrane separation performance dropped drastically with increase in temperature and it turned to be H<sub>2</sub>-selective with H<sub>2</sub>/CO<sub>2</sub> separation selectivity of only 2 at 200 °C (Hong *et al.*, 2008). Therefore, modification on the SAPO-34 zeolite membrane is required to further enhance its affinity toward CO<sub>2</sub>, aims at improving the ability of the membrane for the separation of CO<sub>2</sub> from CO<sub>2</sub>/CH<sub>4</sub>, CO<sub>2</sub>/N<sub>2</sub> and CO<sub>2</sub>/H<sub>2</sub> gas mixtures, even at high temperature. Ion-exchange with different cations is among the methods that can be used to modify the SAPO-34 surface properties. There have been several studies reported for ion-exchange of SAPO-34 molecular sieve in the literature. Li *et al.* (2009) has studied the ion-exchange of SAPO-34 molecular sieve using cations Mg<sup>2+</sup>, Ca<sup>2+</sup>, Sr<sup>2+</sup> and Ba<sup>2+</sup> aimed at improving the methanol conversion to light olefin. On the other hand, ion-exchange of SAPO-34 molecular sieve with cations such as Ce<sup>3+</sup>, Ti<sup>2+</sup>, Mg<sup>2+</sup>, Ca<sup>2+</sup>, Ag<sup>+</sup>, Na<sup>+</sup> and Sr<sup>2+</sup> was found to change the properties of the molecular sieve including its pore width, surface area and light gases adsorption capability (Rivera-Ramos and Hernández-Maldonado, 2007; Rivera-Ramos *et al.*, 2008). Hence, the effect of modification (ion-exchange) towards CO<sub>2</sub> separation performance of the SAPO-34 zeolite membrane needs to be investigated in the present study.

There is no optimization study reported in the literature related with the process variables for gas permeation and separation using SAPO-34 zeolite membrane. The conventional approaches in the gas permeation and separation studies were conducted by running large number of experiments with only one process variable varied at a time. It is difficult to evaluate the possible interactions between the process variables by performing this one-factor-at-a-time approach (Montgomery, 2009). It is highly desirable to apply the statistical approach to determine the optimum conditions in permeation and separation studies of different gas mixtures containing CO<sub>2</sub>, by performing minimum numbers of experiment runs. Design of experiment (DOE) is a useful statistical tool with its ability to evaluate the interactions between process variables, in addition to identification of optimum conditions for the membrane separation processes in order to maximize the flux and separation selectivity.

Mathematical models help in the better understanding of the transport phenomenon of different gas molecules through SAPO-34 zeolite membrane. The models should be able to predict the CO<sub>2</sub> permeation and separation performance of SAPO-34 membrane, in terms of gas fluxes, permeances and separation selectivity, for different gas mixtures. Determination of constants (i.e. adsorption constants and diffusivities) significantly helps in better understanding toward mechanisms of CO<sub>2</sub> permeation and separation in different gas mixtures. These models can be simulated and the simulated results could be compared with the experimental data in order to validate the models. The predictive models for CO<sub>2</sub> gas permeation and separation performance over wide range of process variables will be a useful tool in developing scalable membrane-based CO<sub>2</sub> separation technology.

## 1.5 Objectives

The present research aims at achieving the following objectives:

1. To synthesize SAPO-34 zeolite membrane through direct in-situ crystallization and MW heating.
2. To investigate the effect of MW heating time towards the formation of uniform and thin SAPO-34 membrane.
3. To modify the synthesized membrane using ion-exchange process with different cations and characterize the SAPO-34 zeolite membranes synthesized.
4. To study the performance of SAPO-34 membrane for the permeation and separation of CO<sub>2</sub> from CO<sub>2</sub>/CH<sub>4</sub>, CO<sub>2</sub>/N<sub>2</sub> and CO<sub>2</sub>/H<sub>2</sub> binary gaseous mixtures over wide range of process conditions (temperature, pressure difference across the membrane and CO<sub>2</sub> concentration in the feed).
5. To propose mathematical models for the prediction of gas fluxes, permeances and separation selectivities through SAPO-34 zeolite membrane in single gas permeation, binary gas mixture permeation and separation at different operating conditions. To compare the simulated results with the experimental data to verify the validity of the model.

## **1.6 Scope of the Study**

### **1.6.1 Synthesis of SAPO-34 Zeolite Membranes**

The SAPO-34 zeolite membrane was synthesized through direct in-situ crystallization following the procedures reported by Li *et al.* (2004). MW heating was adapted for the formation of SAPO-34 zeolite membranes. The effect of MW heating time (varied within 0.5-3 hours) was investigated towards quality of SAPO-34 zeolite membranes formed. Comparisons, in terms of properties and CO<sub>2</sub> separation performance, were made between the SAPO-34 zeolite membranes synthesized by direct in-situ crystallization and MW heating.

### **1.6.2 Modification of SAPO-34 Zeolite Membranes**

Selected SAPO-34 zeolite membrane was subjected to modification (ion-exchange) with cations Ca<sup>2+</sup>, Mg<sup>2+</sup>, Sr<sup>2+</sup> and Ba<sup>2+</sup>. The modified SAPO-34 zeolite membranes were compared for their properties and CO<sub>2</sub> gas separation from CO<sub>2</sub>/CH<sub>4</sub>, CO<sub>2</sub>/N<sub>2</sub> and CO<sub>2</sub>/H<sub>2</sub> gas mixtures.

### **1.6.3 Characterization of Unmodified and Modified SAPO-34 Zeolite Membranes**

Various techniques were used to characterize the unmodified and modified SAPO-34 zeolites, either in the form of powder or membrane, as presented in Table 1.2. Single nitrogen permeation measurement at 30 °C and 3 bar pressure difference was performed for each coating of SAPO-34 zeolite layer before calcination process to determine the presence of defects in the membrane.

**Table 1.2:** Characterization techniques of SAPO-34 zeolite membrane

<b>Method</b>	<b>Properties</b>
Transmission Electron Microscopy (TEM)	Surface morphology and zeolite pore channel
Selected Area Electron Diffraction (SAED)	Presence of crystalline phase
X-ray Diffraction (XRD)	Crystallinity, structure and orientation
Scanning Electron Microscopy (SEM)	Microstructure, crystal size and membrane thickness.
Thermal Gravimetric Analysis (TGA)	Water content, template content and thermal stability.
Nitrogen Adsorption-Desorption Measurement	Surface area, pore width, micropore and mesopore volume and isotherm.
Fourier Transformed Infra Red (FTIR)	Characteristic framework vibration bands.
Energy Dispersive X-ray Spectroscopy (EDS)	Elemental composition.

#### **1.6.4 Single Gas Permeation, Binary Gas Mixtures Permeation and Separation using SAPO-34 Zeolite Membranes**

All the unmodified and modified SAPO-34 zeolite membranes were subjected to preliminary gas permeation and separation of equimolar CO<sub>2</sub>/CH<sub>4</sub>, CO<sub>2</sub>/N<sub>2</sub> and CO<sub>2</sub>/H<sub>2</sub> binary gas mixtures at 30 °C and 100 kPa. The modified SAPO-34 zeolite membrane with the highest preliminary CO<sub>2</sub> separation performance, was selected for single gas permeation studies of CO<sub>2</sub>, CH<sub>4</sub>, N<sub>2</sub> and H<sub>2</sub> over temperature of 30-180 °C and pressure difference of 100-500 kPa across the membrane. Thorough permeation and separation studies for the CO<sub>2</sub>/CH<sub>4</sub>, CO<sub>2</sub>/N<sub>2</sub> and CO<sub>2</sub>/H<sub>2</sub> binary gas mixtures were carried out using the selected modified SAPO-34 zeolite membrane over temperature of 30-180 °C, pressure difference of 100-500 kPa across

the membrane and 5-50 % CO<sub>2</sub> concentration in the feed. Determination of the ranges of process variables was based on the literature search and on the limitation of experimental membrane separator rig. The ability of the selected modified SAPO-34 zeolite membrane for separating CO<sub>2</sub> from the CO<sub>2</sub>/CH<sub>4</sub>, CO<sub>2</sub>/N<sub>2</sub> and CO<sub>2</sub>/H<sub>2</sub> binary gas mixtures containing CO<sub>2</sub> concentration in the feed as low as 5 %, was explored.

#### **1.6.5 Optimization for Binary Gas Mixtures Permeation and Separation of Modified SAPO-34 Zeolite Membrane using DOE**

DOE was selected for the permeation and separation studies of CO<sub>2</sub>/CH<sub>4</sub>, CO<sub>2</sub>/N<sub>2</sub> and CO<sub>2</sub>/H<sub>2</sub> binary gas mixtures using Design Expert software version 6.0.6 (STAT-EASE inc., Mineapolis, USA). In this statistical method, all variables were varied simultaneously in according to a set of experimental runs generated by Design Expert software. Response surface methodology (RSM) coupled with central composite design (CCD) was used to optimize the process variables for the CO<sub>2</sub> permeation and separation performance. Model equations were determined using quantitative data from the set of experimental runs. The effect of interaction between the process variables toward the responses was analyzed and the responses were optimized.

#### **1.6.6 Modeling for Single Gas Permeation, Binary Gas Mixture Permeation and Separation of Modified SAPO-34 Zeolite Membrane**

The single gas permeation, binary gas mixture permeation and separation of selected modified SAPO-34 zeolite membrane were modeled on the basis of combined effect of adsorption and diffusion. The adsorption and diffusion constants determined from the gas permeation data, were incorporated into the models. Single

gas fluxes, single gas permeances of different gas molecules ( $\text{CO}_2$ ,  $\text{CH}_4$ ,  $\text{N}_2$ ,  $\text{H}_2$ ) and the ideal selectivities (determined for single gas permeations) were modeled for temperature of 30-180 °C and 100-500 kPa pressure difference across the membrane. Models were also built to represent the gas fluxes, gas permeances and separation selectivities for equimolar  $\text{CO}_2/\text{CH}_4$ ,  $\text{CO}_2/\text{N}_2$ ,  $\text{CO}_2/\text{H}_2$  binary gas mixture permeation and separation through selected modified SAPO-34 zeolite membrane at 30-180 °C and 100 kPa pressure difference across the membrane.

## **1.7 Organization of Thesis**

In the first chapter (Introduction), the definition of zeolite membrane is introduced. Current issue of  $\text{CO}_2$  and the approaches, including the membrane-based technologies, available for  $\text{CO}_2$  separation are presented. The problem statements are elaborated, followed by determination of objectives and scope of study for present research project.

In the second chapter (literature review), reviews on the methods for synthesis of zeolite membranes, in addition to the modification approach for zeolite membranes, are presented. Characterization techniques used for analysis of chemical and physical properties of the zeolite membranes are elaborated. The gas permeation and separation studies reported for different zeolite membranes are discussed. At the end of this chapter, reviews of modeling and simulation process study for zeolite membranes are presented.

Chapter three (materials and methods) presents the list of all materials and chemicals used in present research project. Detailed procedures for the synthesis and modification of SAPO-34 zeolite membranes are presented. This chapter presents

the preparation of SAPO-34 zeolite sample for various characterization techniques. Operating procedures of the gas permeation and separation test rig in measuring the gas permeation and separation, gas sample collection and analysis are elaborated.

In the fourth chapter (results and discussion), the experimental results are presented and discussed. Firstly, the characterizations of unmodified and modified SAPO-34 zeolite membranes are presented. This is followed by preliminary equimolar binary gas mixture permeation and separation through SAPO-34 zeolite membranes. The selected modified SAPO-34 zeolite membrane was subjected to thorough single gas permeation of CO<sub>2</sub>, CH<sub>4</sub>, N<sub>2</sub> and H<sub>2</sub>, followed by permeation and separation studies of CO<sub>2</sub>/CH<sub>4</sub>, CO<sub>2</sub>/N<sub>2</sub> and CO<sub>2</sub>/H<sub>2</sub> binary gas mixtures. In the next section, DOE approach was used to determine the effect of interaction between process variables towards the responses and optimization of the responses. At the last section, modeling studies for the single gas permeation (CO<sub>2</sub>, CH<sub>4</sub>, N<sub>2</sub> and H<sub>2</sub>), binary gas mixture (CO<sub>2</sub>/CH<sub>4</sub>, CO<sub>2</sub>/N<sub>2</sub> and CO<sub>2</sub>/H<sub>2</sub>) permeation and separation are presented. The models were built to predict the gas fluxes, gas permeances and separation selectivities through selected modified SAPO-34 zeolite membrane. The validity of the models was determined by performing comparison between simulated and experimental results.

Chapter 5 (conclusions and recommendations) presents the conclusive attainment of the major findings in the present study. Suggestions and recommendations are presented as improvement for the present study in the future.

## CHAPTER 2

### LITERATURE REVIEW

#### 2.1 Synthesis of Zeolite Membrane

The formation and properties of the zeolite products depend on large number of parameters, such as the synthesis conditions (i.e. temperature, pressure, stirring) and the compositions of the precursor solution required for synthesis (i.e. ratio between elements for framework formation, pH, content of the structure directing agent, water concentration) (Cubillas and Anderson, 2010). Figure 2.1 presents the phenomenon occurrence from nutrients to formation of zeolite crystals. The synthesis of zeolite starts with preparation of precursor solution consisting of required nutrients such as element for framework formation (Si, Al, P, O) and structure directing agent (SDA). By heating the precursor solution to desired temperature at autogenic pressure in an autoclave, entities with different size are formed through hydrolysis, oligomerization and condensation reactions catalyzed by hydroxyl ions. The amorphous phase is formed and is at pseudo-equilibrium with solution phase. After a period, breaking and remaking Si,Al-Si,Al bonds by the hydroxyl ions, results in formation of nuclei and followed by zeolite crystals (Cundy and Cox, 2005). Simultaneously, transformation of the amorphous phase into crystalline phase or dissolution of the amorphous phase into more stable product could happen. The zeolite crystals formed then grow with time in the autoclave (Coronas, 2010; Cubillas and Anderson, 2010).

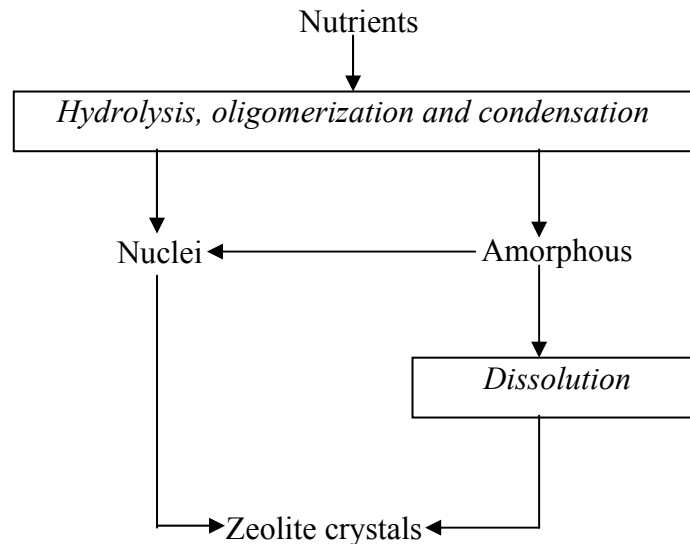


**Figure 2.1:** Phenomenon occurrence for transformation of nutrients into zeolite crystals (Coronas, 2010)

### 2.1.1 Methods of Zeolite Membrane Synthesis

There are numbers of report in the literature for the preparation of different types of zeolite membranes. These zeolite membranes includes MFI (ZSM-5 and silicalite-1), FAU (NaX and NaY), DDR, T-type, SAPO-34 and medernite membranes (Snyder and Tsapatsis, 2007). Figure 2.2 shows the common strategies being reported for the preparation of zeolite membranes in the literature. The thin zeolite membrane can be formed on top of a selected porous support using different techniques: (1) Liquid phase synthesis (direct in-situ crystallization and secondary (seeded) growth method) and (2) vapor phase synthesis (vapor phase transformation and steam-assisted crystallization).

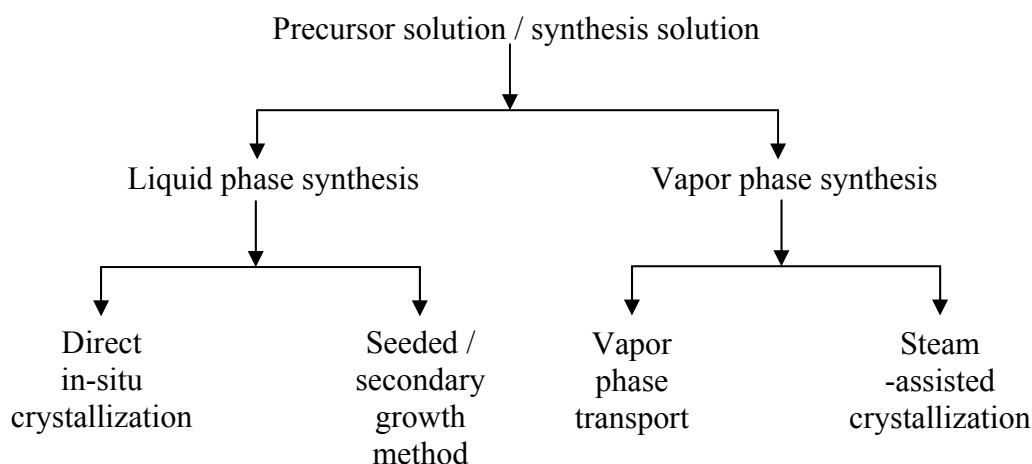


**Figure 2.2:** General methods for synthesis of zeolite membranes (Caro *et al.*, 2000)

The differences in the preparation of zeolite membranes following different methods are illustrated in Figure 2.3. In direct in-situ crystallization, the support is immersed in a precursor solution with known concentration under hydrothermal condition at given temperature. In secondary (seeded) growth method, a closely packed layer of zeolite crystal seeds is deposited onto the surface of a support before crystallization. Different techniques for the deposition of zeolite seeds on the support surface are reported in the literature such as rubbing, dip coating, slip casting and vacuum seeding. Subsequent hydrothermal synthesis is carried out to decouple the nucleation step and crystal growth (Pina *et al.*, 2004). Vapor phase synthesis is another method for the synthesis of zeolite membrane. The precursor is coated on the support via dipping technique, followed by drying. The dry, amorphous precursor is converted to crystalline material via contact with the vapor phase of an organic-water mixture (Parvelescu *et al.*, 2007).

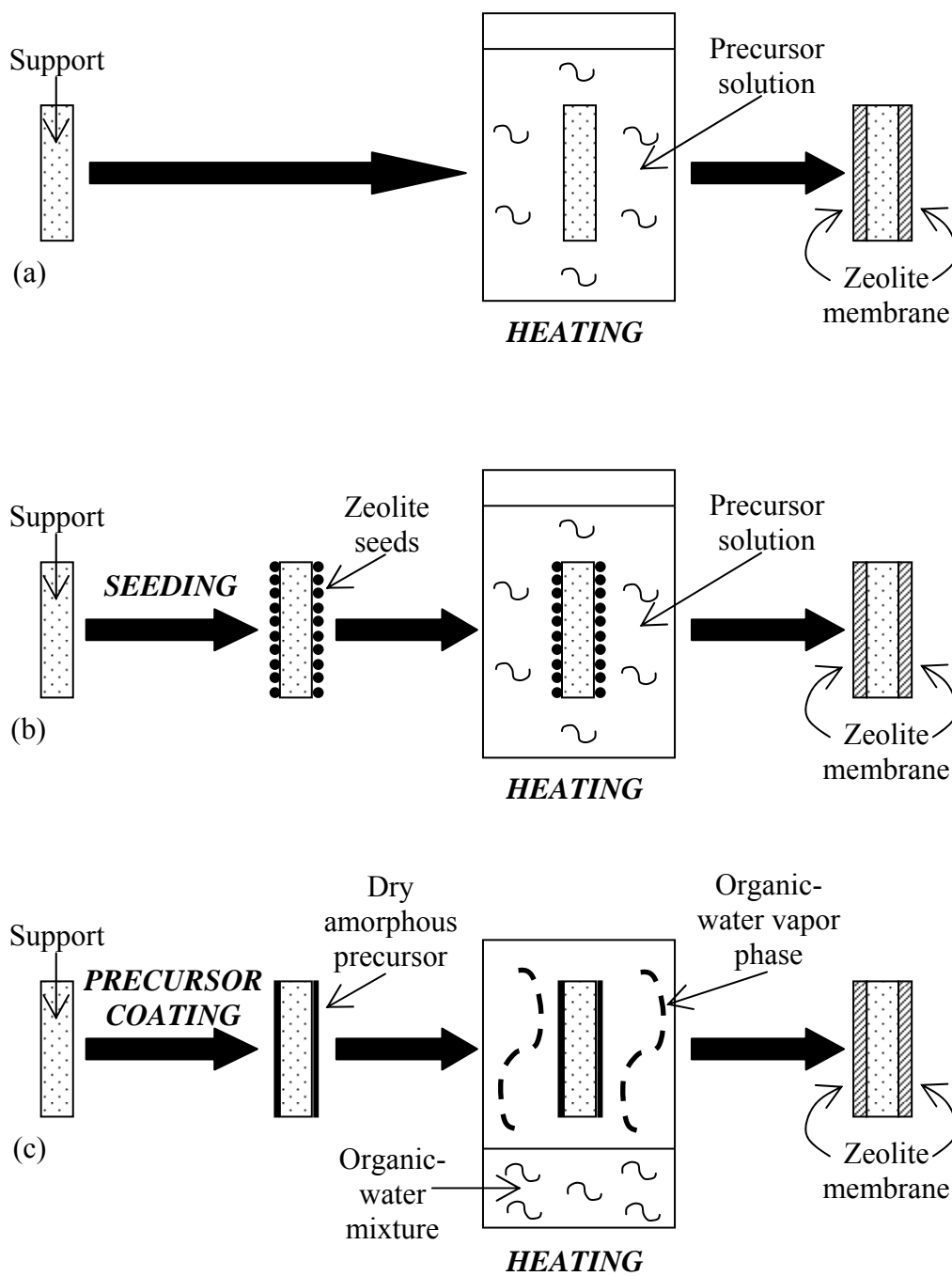


**Figure 2.3:** Steps in the preparation of zeolite membranes on double side of disc-shaped support for different methods: (a) direct in-situ crystallization hydrothermal synthesis, (b) secondary growth (seeded) hydrothermal synthesis and (c) vapor phase synthesis